*AJNR Am J Neuroradiol* 21:1559–1562, September 2000

**Case Report**

# Amyloidoma of the Skull Base

William A. Simoens, Luc van den Hauwe, Eddy Van Hedent, Fabienne Warson, Roland Demaeseneer, David Williams, and Arthur M.A. De Schepper

**Summary: We report a case of a primary amyloidoma of the skull base. Plain radiography and CT showed a lytic, highly destructive lesion with multiple scattered calcifications within. MR imaging revealed that the tumor was iso- to hypointense to muscle on T1-weighted images and extremely hypointense on T2-weighted images. In contrast to two previous reports, marked enhancement after the administration of contrast material was absent. Bone amyloidomas are very rare and are frequently misinterpreted as chondrosarcomas.**

Amyloidomas are tumors consisting of localized deposits of amyloid, an insoluble, fibrillar proteinaceous material (1), and are the rarest form in the group of amyloidosis-related pathologic abnormalities. They occur most frequently in the upper respiratory tract and nasal sinuses and less frequently in sites such as lung, skin, lower urinary tract, tongue, gastrointestinal tract, breast, brain, and soft tissues (2).

The skeleton, in particular the skull base, is involved very rarely, and often amyloidomas of the bone are misinterpreted radiologically as chondrosarcomas (2–6). We report a case of a primary amyloidoma of the skull base, seen on plain radiographs, CT scans, MR images, and nuclear scintiscans, with enhancement characteristics different from those described in previous reports.

## Case Report

A 54-year-old Caucasian man consulted his otorhinolaryngologist because of plugging of his right external ear. The patient had undergone surgery for inflammatory maxillary sinus disease at the age of 12 years. Further personal and familial medical histories were not relevant.

After removing the ear plug, the physician noticed that the bony floor of the external ear was denuded of cutis and subcutis and that the bone had a brittle aspect. Cardiac and pulmonary auscultation revealed no abnormalities. The results of a fundus examination of the eye were normal, and no vision disturbances were noted. Osteomyelitis secondary to otitis media was suspected, and the patient was referred to the department of radiology.

Plain radiography of the skull showed destruction of the skull base with erosion of the apex of the right petrous pyramid and the presence of a large number of amorphous dense structures resembling calcifications. The right occipital condyle was ill defined when compared with the left one (not shown).

Subsequent CT showed abnormal bone extending along the right petro-occipital and petroclival synchondrosis. There was replacement of the normal bone of the clivus, right occipital condyle, and right petrous apex. Scattered within the mass, a myriad of radiodense fragments was noted (Fig 1A and B). It was not clear whether these were calcifications within the tumoral matrix or remnants of fragmented bone. Extension into the sphenoid sinus was noted, with a soft-tissue component interspersed with multiple dense fragments of bone. There were no other signs of inflammatory sinus disease revealed by CT. Interruption of the bony contours of the carotid canal was noted bilaterally. On the right side, an irregular lining of the floor of the external ear was observed. There was no contiguity between the central skull base lesion and the changes in the external auditory canal.

MR imaging revealed the presence of a mass centered on the basiocciput, measuring 4 cm in length and 2.5 cm in width. The mass was clearly extending into the lumen of the sphenoid sinus, but it did not appear to invade the cavernous sinus or Meckel's cavum. As with CT, no signs of active sinusitis were revealed.

The structure was iso- to hypointense to muscle on T1-weighted images (Fig 1C and D) and displayed an extremely hypointense homogeneous signal on T2-weighted images (Fig 1E). After the IV administration of contrast material, only a poorly localized enhancement could be seen (Fig 1F). On MR images, the carotid syphon and hypophysis appeared normal.

Bone scintigraphy (technetium-99m-methylene diphosphate), revealed pathologic bone remodeling of the skull base, predominantly on the right side. The differential diagnosis included chondrosarcoma, chondroid chordoma, lymphoma, and plasmocytoma. Full blood count revealed only a slight leucocytosis. Sedimentation and C-reactive protein dosage were within normal ranges. Immunohistochemistry was normal. Biochemistry showed a hypercholesterolemia of 313 mg% (normal, 150–250 mg%). Parathormone was 22.1 pg/mL (normal, 13–54 pg/mL), alkaline phosphatases were 129 U/L (normal, $<270$), total calcium was 4.74 mEq/L (normal, 4.25–5.2 mEq/L), and plasma creatinine was 1.26 mg% (normal, 0.7–1.3 mg%). Protein dosage on urine revealed no abnormalities. Bence-Jones electroforesis and $\kappa$ and $\lambda$ dosages were normal.

Bone marrow puncture showed a normal maturation of the stem cells of the hematopoietic system. No cells suggestive of malignancy were found. Typing of WBC was normal.

A transseptal sphenoidotomy was performed for biopsy. The ethmoid bone was resected together with the vomer, and the anterior walls of the right and left sphenoid sinuses were resected. After resection of the intersphenoidal septum, a crumbly, yellow-colored mass was found in the sphenoidal sinus.

Received September 22, 1999; accepted after revision February 15, 2000.

From the Departments of Radiology (W.A.S., E.V.H.), Pathology (F.W.), Internal Medicine (R.D.), and ENT (D.W.), Algemeen Stedelijk Ziekenhuis Campus Aalst, Aalst, and the Department of Radiology (W.A.S., L.v.d.H., A.M.A.D.S.), Universitair Ziekenhuis Antwerpen, University of Antwerp, Antwerp, Belgium.

Address reprint requests to William A. Simoens, University Hospital Antwerp, UZA, Wilrijkstraat 10, 2650 Edegem, Belgium.

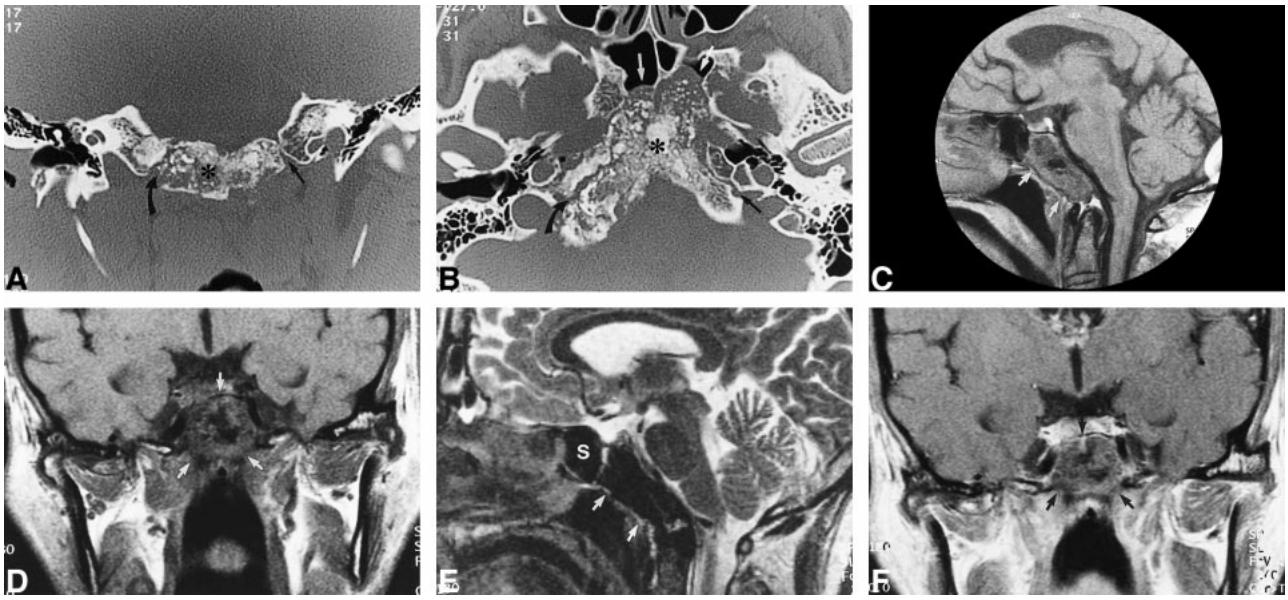


FIG 1. Images from the case of a 54-year-old man with primary skull base amyloidoma.

*A,* High-resolution coronal temporal bone CT scan shows a permeated aspect of the normal bone of the basiocciput, with scattered foci of calcifications or remnants of destructed bone within. The lesion (*asterisk*) is centered on the right petro-occipital fissure (*curved black arrow*) and crosses the midline. The petro-occipital fissure on the opposite side (*straight black arrow*) is intact.

*B,* High-resolution axial temporal bone CT scan. A soft-tissue component (*white arrows*) extends through the posterior wall of the sphenoid sinus.

*C,* Sagittal spin-echo T1-weighted (840/12/3 [TR/TE/excitations]) MR image displays the lesion (*arrows*) as iso- to hypointense to muscle.

*D,* Coronal spin-echo T1-weighted (840/12/3) MR image.

*E,* Sagittal turbo spin-echo T2-weighted (4416/128/1) MR image shows the lesion affecting the clivus (*arrows*) with very low signal intensity, similar to that of the air in the sphenoid sinus (*S*).

*F,* Coronal contrast-enhanced spin-echo T1-weighted (840/12/3) MR image shows poor localized contrast enhancement (*arrows*).

A septum reconstruction was performed using free cartilage and bone grafts.

Microscopically, Congo red stain showed amyloid deposits resistent to potassium permanganate (Fig 2). No signs of fungi were found. To rule out the possibility of systemic amyloidosis, biopsy of the rectal mucosa and submucosa was performed. No amyloid deposits in these locations, which would have suggested systemic amyloidosis, were noted. The final diagnosis was primary amyloidoma of the skull base.

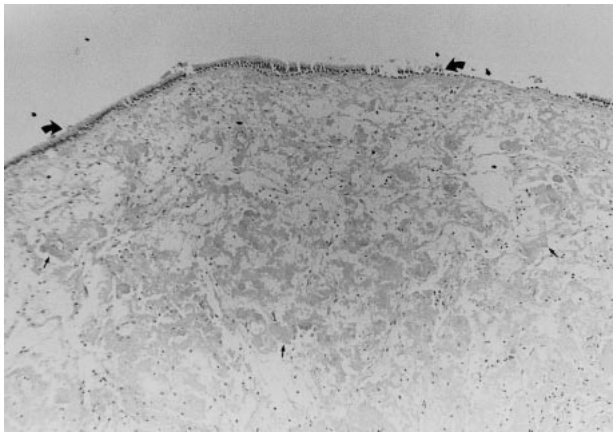

FIG 2. Microscopic image. Congo red staining of the mass found in the sphenoidal sinus shows a marked thickening of the mucosa due to deposits of amyloid presenting as dark amorphous structures (*arrows*). The ciliary epithelium is well shown (*curved arrows*).

## Discussion

Solitary amyloidoma not associated with multiple myeloma is a rare entity (2). To our knowledge, only 37 cases have been reported during the last 100 years (2, 7–9). Little emphasis has been placed on the presentation of amyloid tumors of the skull on medical images in world literature. The mean age at diagnosis is 57.5 years, with a male predominance of 2:1. The spine is affected most frequently (18 of 37 cases). In seven cases, the skull is involved. The preferential involvement of skull and spine is responsible for the predominantly neurologic symptoms reported.

It is well accepted that most, if not all, amyloidomas of bone, and possibly also those of soft tissues, represent plasmocytomas with massive amyloid deposition. These plasmocytomas can be solitary or they may form part of multiple myeloma. This hypothesis is supported by several facts. First, the overall majority of amyloidomas are caused by the deposition of AL-type of amyloid fibrils. Second, monoclonality in the lympohoid/plasma cell infiltrate is shown and plasmocytoma of bone can be associated with monoclonal gammopathies (10). Third, amyloidomas and plasmocytomas share similar locations and patient demographics. Exuberant amyloid production as a manifestation of a plasmacytoma is rare but has been reported (10). Frequent progression to multi-

ple myeloma in the few patients with adequate follow-up has been noted (2), although other investigators claim the opposite (11).

On plain radiographs, the lesions are seen as destructive lytic masses with internal areas of calcification (2). CT findings (3, 6, 7) indicate a lytic, destructive, hypodense, somewhat expansive mass with nodular calcifications. Marked enhancement is typical. On the basis of plain radiographic and CT findings, the possibility of a chondrosarcoma arising along the petro-occipital synchondrosis is often considered, as it was in our case. Ünal et al (6) reported a skull base amyloidoma that was spontaneously hyperdense on CT scans. Marked enhancement of the tumoral mass was noted after the IV administration of iodinated contrast material in all reported cases. However, in our case, only mild enhancement of the tumoral mass was noted after the IV administration of contrast material.

To the best of our knowledge, the MR characteristics of skull base amyloidomas have been reported by only two groups of investigators (6, 7). Both report a heterogeneous mass with areas of low signal intensity on T1- as well as T2-weighted images, probably corresponding to areas of calcification. The cerebral parenchyma was not invaded. Marked enhancement of the mass after the IV administration of contrast material was noted in both cases. The mild contrast enhancement in our case was probably due to the high calcium content of the tumor matrix.

It has been reported that the signal characteristics of amyloid on MR images closely resemble those of skeletal muscle, the structure of amyloid being akin in many ways to the highly organized multilayered, myofibrillar ultrastructure of skeletal muscle (12). This may be an important differentiating point: muscle is an easy reference frame, and tumors do not appear in this manner on MR images. Most neoplasms have a more fluid structure than that of amyloid and skeletal muscle and thus tend to brighten on T2-weighted images. Other reports of amyloidosis, focal or systemic, describe this loss of signal intensity on T2-weighted images (13–15). The exact mechanism underlying the signal hypointensity of amyloid on the long-TR images is complex and uncertain. Gean-Marton et al (15) suggested that the unique structure of amyloid, the $\beta$-pleated sheath, potentially plays a role in several ways. First, enhanced T2 decay may result from static or slowly fluctuating internal magnetic fields within adjacent amyloid protons held in fixed positions within the folded protein. These magnetic fields generate local field inhomogeneities, causing the protons to precess at slightly different frequencies. The protons therefore lose phase coherence, transverse magnetization, and, consequently, T2 signal intensity. Moreover, the configuration of this proton is unusual, allowing it to pack more densely, and therefore exclude water, than do proteins with a more globular quaternary structure. Second, rapid chemical exchange and spin-spin interactions may occur between the amyloid protein and adjacent water molecules. In chemical exchange, an ''in-phase'' outside water proton is substituted for a ''dephased'' proton within the amyloid protein. In spin-spin interaction, energy, but not the actual proton, from a surrounding water proton is exchanged with energy from a spin on the amyloid protein. Unlike chemical exchange, no physical exchange of matter occurs in spin-spin interaction. In both cases, the exchange leads to loss of phase. Because dephased protons are not imageable, a loss of signal intensity occurs. Finally, the amyloid microenvironment is composed of a heterogeneous micromagnetic mixture of collagen, calcification, and vessels as well as the amyloid fibrils. The T2 hypointensity may result from differences in diamagnetic susceptibility. Proton diffusion within the voxel across these intrinsic gradients during interecho time causes their phases to spread out, resulting in an irreversible reduction in transverse magnetization.

The low signal intensity of the mass can thus help to differentiate amyloidoma from other tumors, such as chondrosarcomas, because the latter characteristically exhibit a high signal intensity on T2-weighted images (16). In addition to chondrosarcoma, differential diagnoses should also include chordoma, sinonasal lymphoma, and plasmocytoma. Craniovertebral chordoma is typically located on the midline because it arises from remnants of the embryonic notochord, the terminus of which is in the sphenoid bone, inferior to the sella turcica. Both chondrosarcoma and chordoma have a high signal intensity on T2-weighted images, differentiating them from primary amyloidoma (16). Sinonasal lymphoma presents on CT scans and MR images as a bulky soft-tissue mass, enhancing to a moderate degree. These tumors remodel rather than erode the adjacent bony structures and tend to have an intermediate signal intensity on all MR images. Although it is suggested that amyloidomas of bone and of soft tissues represent plasmocytomas with massive amyloid deposition (10), plasmocytomas tend to have imaging characteristics that are somewhat different from those of the amyloidoma in our patient. Extramedullary plasmocytomas are homogeneous on CT scans and have intermediate signal intensity on all MR imaging sequences. Because they are highly vascular, extramedullary plasmocytomas enhance and may show vascular flow voids on MR images (17). In our patient, no blood or bone marrow abnormalities were found that could suggest the existence of lymphoma or plasmocytoma. The intermediate signal intensity that lymphoma and plasmocytoma usually exhibit allows them to be discerned from amyloidoma, as in our case, which showed very low signal intensity, especially on T2-weighted images. Additionally, the lack of enhancement of the amyloidoma in our case is not typical for lymphoma nor plasmocytoma.

Biopsy of the lesions in the external auditory canal was never performed, and thus, we cannot ex-

clude the possibility of a second focus of amyloidoma. A conservative approach to the lesion was adopted, but unfortunately, the patient was lost to follow-up.

## Conclusion

Despite the rarity of primary amyloidomas of the skull base and despite the nonspecificity of imaging findings regarding this entity, which is often mistaken for a chondrosarcoma on plain radiographs and CT scans, this tumor should be considered in the differential diagnosis of a skull base tumor, especially when resembling a chondrosarcoma. An important clue to its diagnosis can be the remarkably low signal intensity on T2-weighted images of amyloidoma, which distinguishes it from chondrosarcoma and craniovertebral chordoma.

## References


1. Cohen AS, Calkens E. **Electron microscopic observations on a fibrous component in amyloid of diverse origins.** *Nature* 1959; 183:1202–1203
2. Pambuccian SE, Horyd IDH, Cawte T, Huvos AG. **Amyloidoma of bone, a plasma cell/plasmacytoid neoplasm: report of three cases and review of the literature.** *Am J Surg Pathol* 1997;21: 179–186
3. Ferreiro JA, Bhuta S, Nieberg RK, Verity MA. **Amyloidoma of the skull base.** *Arch Pathol Lab Med* 1990;114:974–976
4. Giordano A, Horne DG, Gudbrandsson F, Meyerhoff W. **Temporal bone amyloidoma.** *Otolaryngol Head Neck Surg* 1983;91: 104–108
5. Bürgi U. **Über einen Fall von solitarem Amyloidtumor des Scheitelbeins.** *Frankf Z Pathol* 1937;50:410–428
6. Ünal F, Hepgül K, Bayindir C, Bilge T, Imer M, Turantan I. **Skull base amyloidoma: case report.** *J Neurosurg* 1992;76:303–306
7. Hidalgo F, Aguilera C, Monfort JL, René M, Muntané A, Pons LC. **Amyloidoma of the skull: plain radiographs, CT and MRI.** *Neuroradiology* 1996;38:44–46
8. Dee CH, Missirian RJ, Chernoff IJ. **Primary amyloidoma of the spine: a case report and review of the literature.** *Spine* 1998; 23:497–500
9. Porchet F, Sonntag VKH, Vrodos N. **Cervical amyloidoma of C2: case report and review of the literature.** *Spine* 1998;23:133–138
10. Wiltshaw E. **The natural history of extramedullary plasmacytoma and its relation to solitary myeloma of bone and myelomatosis.** *Medicine (Baltimore)* 1976;55:217–238
11. Lipper S, Kahn LB. **Amyloid tumor: a clinicopathologic study of four cases.** *Am J Surg Pathol* 1978;2:141–145
12. Banker BQ, Girvin JP. **The ultrastructural features of the mammalian muscle spindle.** *J Neuropathol Exp Neurol* 1971; 30:155–195
13. Rafal RB, Jennis R, Kosovsky PA, Markisz JA. **MRI of primary amyloidosis.** *Gastrointest Radiol* 1990;15:199–201
14. Sueoka BL, Kasales CJ, Harris RD, Heaney JA. **MR and CT imaging of perirenal amyloidosis.** *Urol Radiol* 1989;11:97–99
15. Gean-Marton AD, Kirsch CF, Vezina LG, Weber AL. **Focal amyloidosis of the head and neck: evaluation with CT and MR imaging.** *Radiology* 1991;181:521–525
16. Curtin HD, Som PM, Braun IF, Nadel L. **Skull base.** In: Som PM, Curtin HD, eds. *Head and Neck Imaging.* 3rd ed. St. Louis: Mosby; 1996:1233–1299
17. Som PM, Brandwein M. **Sinonasal cavities: inflammatory diseases, tumors, fractures and postoperative findings.** In: Som PM, Curtin HD, eds. *Head and Neck Imaging.* 3rd ed. St. Louis: Mosby; 1996:126–315